Available online at www.sciencedirect.com
ScienceDirect
Trans. Nonferrous Met. Soc. China 29(2019) 2237−2244
Transactions of Nonferrous Metals Society of China
www.tnmsc.cn

Cooling slope casting of AA7075 alloy combined with reheating and thixoforging

Kerem Altug GULER[1], Alptekin KISASOZ[1], Gokhan OZER[2], Ahmet KARAASLAN[1]

1. Department of Metallurgical and Material Engineering, Yildiz Technical University, TR34210, Istanbul, Turkey;
2. Aluminium Test, Training and Research Center (ALUTEAM), Fatih Sultan Mehmet Vakif University, TR34445, Halic Campus, Istanbul, Turkey

Received 22 February 2019; accepted 4 July 2019

Abstract: Cooling slope casting has been applied to aluminium casting alloys for producing ingots with non-dendritic microstructure. Semi-solid forming of the AA7075 was studied via cooling slope casting, reheating and thixoforging processes in order to determine the effect of semi-solid casting on the microstructure of the alloy. AA7075 ingots with non-dendritic microstructure were produced with cooling slope pouring. Castings were characterized by light microscopy, image analysis, scanning electron microscopy and EDS analysis. The resulting structures are promising in terms of grain size and sphericity. It was realized that grain coarsening may occur very suddenly in the reheating process. Cooling slope castings were obtained with 30° and 60° inclination angles, and in comparison, 60° castings showed better results. Moreover, by using short reheating periods, semi-solid forging causes trace formation in the solid grains.

Key words: semi-solid alloy; cooling slope casting; thixoforging; AA7075 alloy

1 Introduction

Aluminium alloys possess remarkable engineering properties like low density, high toughness, high specific strength and low cost. The 7xxx series aluminium alloys are widely used in military equipment, automobile, and aerospace industries. AA7075 is the most wildly used alloy in the 7xxx series with superior properties comparable to soft steel. Aluminium alloys are generally fabricated with casting and forging processes [1−6]. The formation of defects and equipment requirements in the casting process, and difficulties of manufacturing thin and complex geometries in the forging process cause several disadvantages in the fabrication of aluminium alloys. Semi-solid metal forming (SSMF) technology combines the advantages of casting and forging processes and eliminates the disadvantages in the fabrication of aluminium alloys [7−10].

SSMF process can be defined as a near-net shape manufacturing route. It exhibits the considerable forming ability and mechanical properties for both steel and non-ferrous alloys. SSMF can be classified into two groups, rheoforming and thixoforming. Thixoformed samples also provide comparable mechanical properties with the forged ones. Non-dendritic, equiaxed and globular grain structure is essential to form aluminium alloys without any defects in a semi-solid state. Desirable microstructural properties for the SSMF of aluminium alloys can be obtained by several manufacturing routes like cooling slope casting (CSC), recrystallization and partial melting (RAP) and strain induced melt activated (SIMA) methods [11−14]. CSC is one of the most widely used processes to produce feedstock for further thixoforming treatment. It involves two main process steps: (1) pouring molten metal through a plate, and (2) solidification of metal in a mould. Non-dendritic and globular grain structure can be obtained by dendritic fragmentation and crystal separation mechanisms. The weak dendrite arms may occur on the contact surface of the cooling slope and molten metal flow through the inclined slope results in the fragmentation of dendrite arms. On the other hand, globular grains nucleate and grow through the cooling slope wall and these grains move into a mould with molten metal flow [15−18].

There are several studies about the manufacturing of

Corresponding author: Alptekin KISASOZ; E-mail: akisasoz@yildiz.edu.tr
DOI: 10.1016/S1003-6326(19)65129-0

AA7075 in semi-solid state by using CSC, RAP and SIMA methods. JAVDANI et al [19] also investigated the semi-solid forming of AA7075/Al_2O_3 composites. MESHKABADI et al [20] combined the ECAP and subsequent heating to semi-solid process temperature for AA7075 and the microstructure of the alloy became more suitable for SSMF. Although semi-solid processing of AA7075 is advantageous for obtaining suitable microstructure, the liquid−solid phase ratio, process temperature and holding time are critical for desired microstructural and mechanical properties. FU et al [21] stated that fracture mode depends on the liquid fraction of the sample for semi-solid processed AA7075. In the study of CHEN et al [22], It was determined that the hot tensile behaviour of AA7075 is governed by both solid and liquid phases between 520 and 550 °C, and above 550 °C, and the liquid phase is dominant for the tensile behaviour at semi-solid state. Another critical case for the semi-solid processing of the AA7075 is grain coarsening occurred during the process. ROKNI et al [23] emphasized that the enhanced semi-solid process temperature induces a grain coarsening and the thickness of the liquid phase at grain boundaries is increasing. MOHAMMADI et al [24] reported that the grain size and morphology of semi-solid processed AA7075 may be influenced by holding temperature and time. The volume fraction of the liquid phase increases with the enhanced process temperature and the globular grains also coarsen at long holding time. FU et al [25] also observed that coalescence is the dominant mechanism for grain coarsening in the early stage of melting and the Ostwald ripening is active for longer holding time for AA7075. JIANG et al [26] compared the microstructural properties of AA7075 fabricated with SIMA and RAP. It was observed that the RAP provides more globular grain structure compared to SIMA and, Ostwald ripening may occur for the SIMA and RAP processes applied at 590 and 600 °C. GUNER et al [27] also reported that the mean size of the grains increases with increasing treatment temperature for the SIMA-processed AA7075. ATKINSON and LIU [28] compared the grain coarsening behaviour of various aluminium alloys for RAP and CSC. It was stated that grain coarsening of AA2014 is more critical in CSC compared with RAP. Although the CSC process is sensitive to grain coarsening, there are limited studies about grain coarsening behaviour of CSC-processed AA7075.

2 Experimental

In the casting process, a 10 mm-thick AA7075 plate supplied from a local supplier was used. The chemical composition of this alloy is given in Table 1. Fragments of the plate in appropriate size were melted in a clay/graphite crucible using an electric-resistant furnace. The melting process was carried out at 660 °C (25 °C above liquidus temperature) and 750 g alloy was melted for each casting. Any grain refinement procedure was not performed during melting. After melting, the liquid metal was poured into a cylindrical steel mould with a diameter of 40 mm through a cooling slope. A copper tube with a length of 650 mm and a diameter of 50 mm was used as a cooling slope. The inside of this tube was coated with hexagonal boron nitride spray to prevent metal adhesion. Separate castings were made by using 30° and 60° inclination angles.

Table 1 Chemical composition of AA7075 (wt.%)

Si	Fe	Cu	Mg	Zn
0.1	0.19	1.53	2.55	5.89
Mn	Cr	Ni	Ti	Al
0.07	0.18	0.0058	0.024	Bal.

Slugs with a length of 40 mm were cut out from ingots and reheated to 615 °C (20 °C below liquidus temperature). A laboratory-type electric-resistant heat treatment furnace was used for the reheating process. Reheating time was determined to be 30, 60 and 90 min, respectively. Two slugs were reheated each time, one of them was quenched and the other was thixoforged with 50% deformation rate in an open die using a hydraulic press.

After these processes, specimens were taken from approximately centre zone of quenched and thixoforged slugs and subjected to metallographic preparation procedures. Keller reagent was used for etching. Basic microstructure observations and measurements were achieved using a light microscope and image analysis. Further observations and EDS analyses were carried out with a scanning electron microscope.

3 Results and discussion

Casting temperatures should be kept within low super heat temperature limits in order to obtain high efficiency from cooling slope castings. The determined casting temperature 660 °C is in low super heat limits for AA7075 and at this temperature, the alloy has enough fluidity that can be completely poured out of the crucible by gravity. Of course, it should not be expected that the high fluidity of the casting alloys comes from the AA7075, which is a wrought alloy. The average ingot mass values obtained in the castings with 30° and 60° slope angles are 572 and 705 g, respectively. In this case, the casting efficiencies are calculated as 76.26% and 94.00%, respectively. During the castings, especially in 30° inclined pouring, a retained thick alloy shell was

observed in the copper tube.

Microstructures of as-cast ingots are shown in Fig. 1 and measured average grain size and grain aspect ratio (d/L, where d is the width of the grain, L is the length of the grain) values are given in Table 2. First of all, cast structures show that for AA7075 the non-dendritic microstructure can be completely obtained by cooling slope casting. There are no dendritic zones in the microstructures and the grain shapes are close to the sphere.

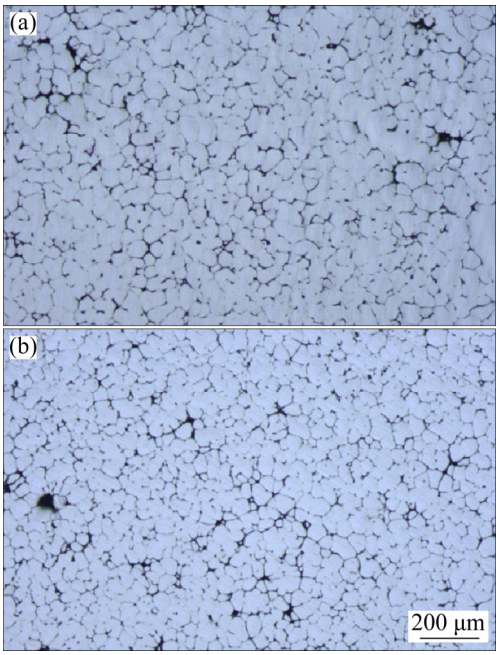


Fig. 1 Microstructures of as-cast ingots at different slope angles: (a) 30°; (b) 60°

Table 2 Grain size and aspect ratio values of as-cast microstructures

Slope angle/(°)	Average grain size/μm	Average aspect ratio, d/L
30°	66	0.82
60°	52	0.80

The grain size of the ingots poured with 60° slope angle is significantly lower than that of 30°. And there is no noticeable difference in aspect ratios. In the 60° slope castings, finer grains are the result of increased shear force due to the high metal flow velocity. In cooling slope castings, grains nucleate and drift on the slope surface. For high process angles, they are naturally subjected to more shear force and ruptures.

When the microstructure images are examined carefully, it is noticed that there are grain coalescences in some regions. This is the case in both but is more obvious in 30° slope castings and it is a reason for increasing grain size. The slow flow in low angle casting increases the accumulation, even these coalescences cause the formation of entrapped porosity. In Fig. 2, some coalescence zones and entrapped porosities are indicated on the microstructure of 30° as-cast ingot microstructure.

In addition, intergranular porosity is seen in microstructures, relatively low fluidity of the alloy and rapid solidification process are the main reasons for this formation.

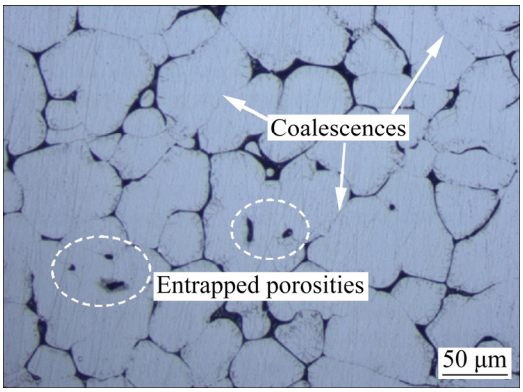


Fig. 2 Indicated coalescence zones and entrapped porosities on 30° as-cast ingot microstructure

In experimental work, reheating temperature was applied at 615 °C. This temperature is just 20 °C below the liquidus point of AA7075 and relatively high in the wide solidification range (158 °C). However, at this temperature, only about 30% liquid is formed [7,22,25].

Microstructures of quenched and thixoforged slugs after reheating are shown in Figs. 3 and 4 at slope angles of 30° and 60°, respectively. The average grain sizes and grain aspect ratios of these structures are given in Fig. 5.

In AA7075, Cr-containing precipitates like $Al_{12}Mg_2Cr$ and $Al_{18}Mg_3Cr_2$ (E-phase) limit grain coarsening and recrystallization by pinning the grain boundaries [29]. It is most likely that these precipitates are not formed as a result of rapid solidification in the casting by the cooling slope. Therefore, the grain growth started before liquefaction and increased dramatically after liquefaction in grain boundary zones.

In this coarsening process, both the grain coalescence and the Ostwald ripening mechanisms are effective. JIANG et al [26] worked with the SIMA and RAP processes on the AA7075 and mentioned the presence of these two growth mechanisms in the semi-solid heating. Most of the grain coarsening took place in the first half-hour of reheating sequence. Reheating to the relatively high temperature, a liquid network was rapidly formed at the grain boundaries and this accelerated grain coarsening. The liquid zones, which form during reheating process, can be observed in microstructures as dark areas at grain boundaries and

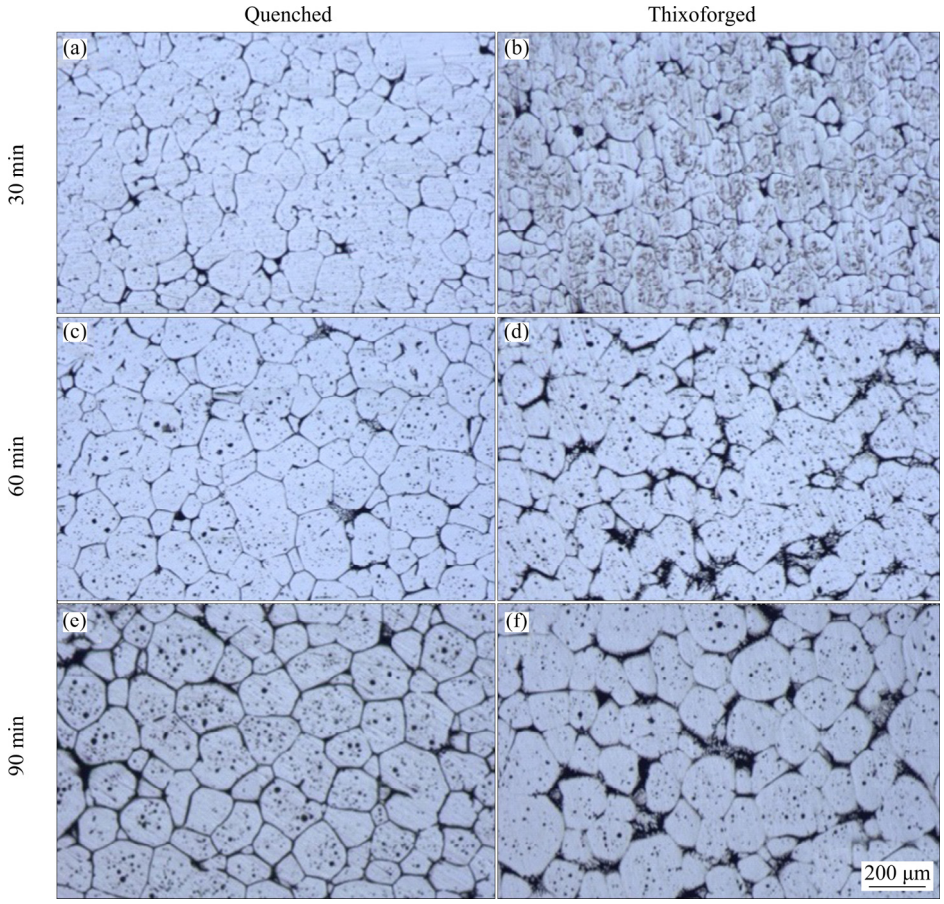


Fig. 3 Microstructures of quenched and thixoforged slugs cast with slope angle of 30°

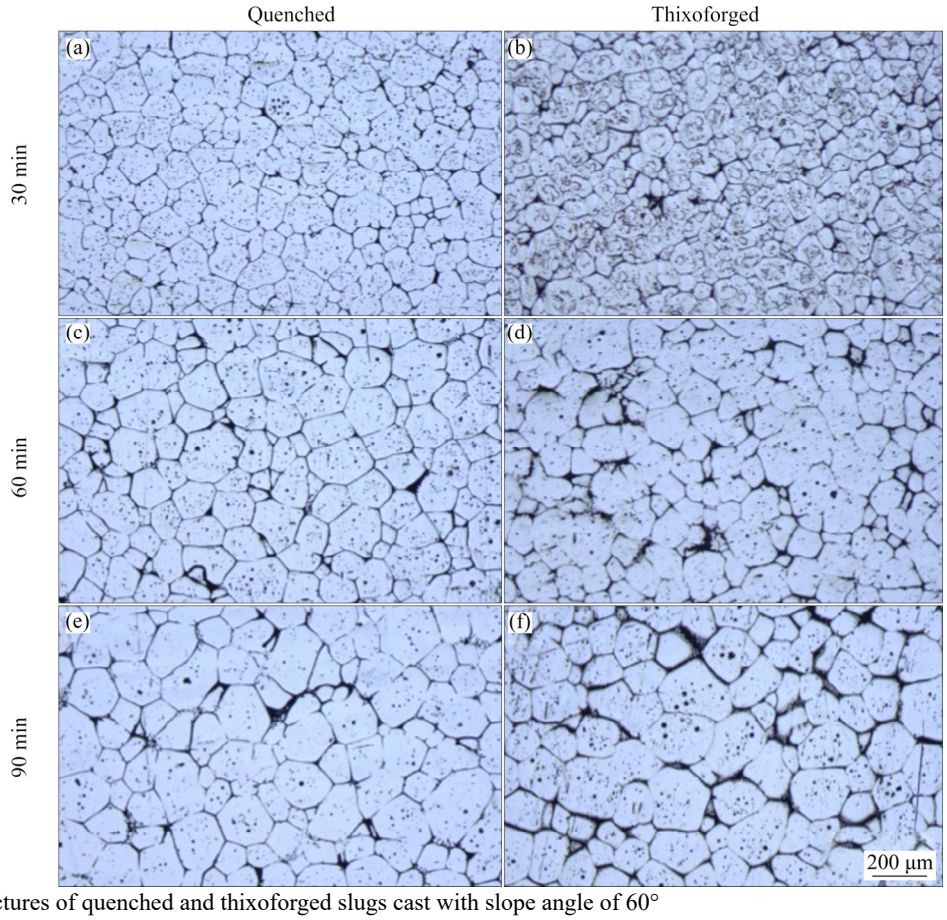


Fig. 4 Microstructures of quenched and thixoforged slugs cast with slope angle of 60°

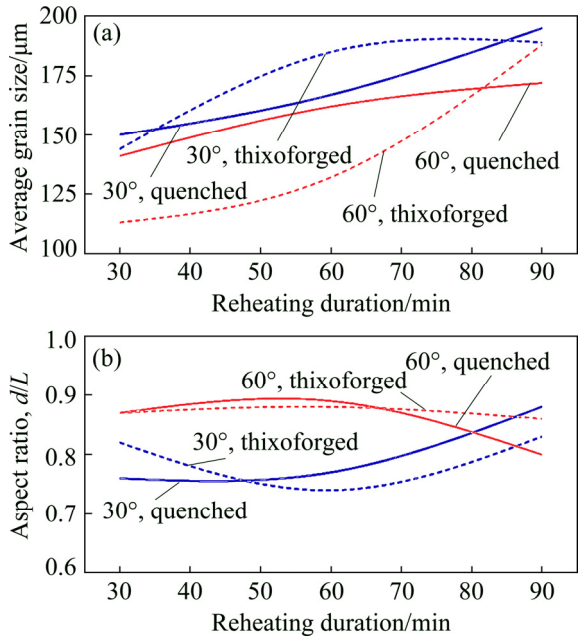


Fig. 5 Average grain size (a) and grain aspect ratio (b) values of slug microstructures

spherical black spots in the grains. These spots are entrapped liquids formed by grain coalescence. Figure 6 illustrates these liquid regions in a high magnification microstructure image. Due to the increase in the holding time at the reheating temperature, the liquid zone is markedly increased. This increase is also the result of coalescence with liquid migration as well as an increase in the total amount of liquid. In the thixoforged samples, the liquid regions appear to be wider, the open die forging extends these areas because of liquid spray. There is no significant difference in grain size at the end of reheating of 30° and 60° slope castings. In the slugs from both castings, grain coarsening happens in a close range. In the evaluation of grain aspect ratios, it can be said that grains of the slugs from 60° slope casting are a little closer to the sphere.

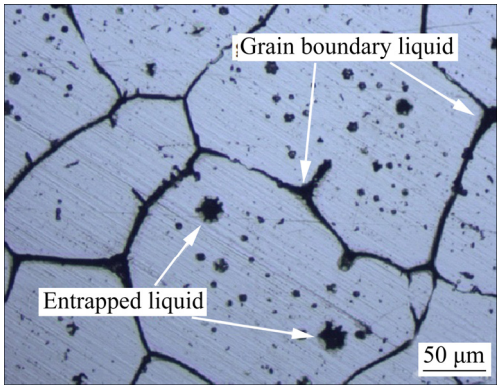


Fig. 6 Liquid zones in microstructure of reheated specimen (cast with 30° slope angle and reheated for 90 min)

The microstructures of the thixoforged samples show that the forging has no significant effect on both grain structure and shape. During deformation, mostly the liquid phase flowed through the solid grains. However, after 30 min of reheating the thixoforged slugs have remarkable traces in the inside of the grains. These traces are observed in the samples from both castings.

AA7075 contains Zn, Mg and Cu as the main alloying elements according to the amount of contents. Considering other trace elements, the chemical structure of this alloy is quite complex. It should not be expected that the liquid formed in the reheating process of such an alloy is homogeneous with the present solid and original of the alloy composition. EDS mapping analysis was performed on the thixoforged specimen which was cast with 60° slope angle and reheated for 30 min. Results of this analysis can be seen in Fig. 7. The liquid regions formed during the reheating process are rich in Cu, while the Al content is rather lower than the average. And there is no great difference between the amounts of Zn and Mg. FU et al [25] studied ECAP (equal-channel angular pressing) based SIMA process of AA7075 and reported critical segregation of Cu and slight segregation of Mg and Zn at grain boundaries during semi-solid heating. Mg and Zn are easily dissolved in Al grains, and

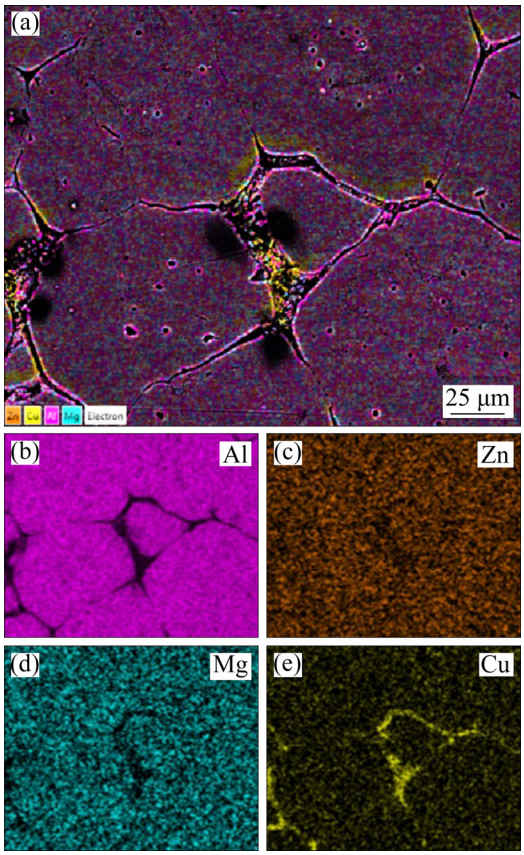


Fig. 7 SEM image (a) and EDS mapping analysis (b−e) of thixoforged specimen cast with 60° slope angle and reheated for 30 min

generally Cu has segregation tendency to the grain boundaries.

In the microstructures of only 30 min reheated, 60° slope angle, and semi-solid shaped samples, the traces appearing inside the grains are unusual. These traces are found to be more closely with the light microscope and SEM, and images are given in Fig. 8.

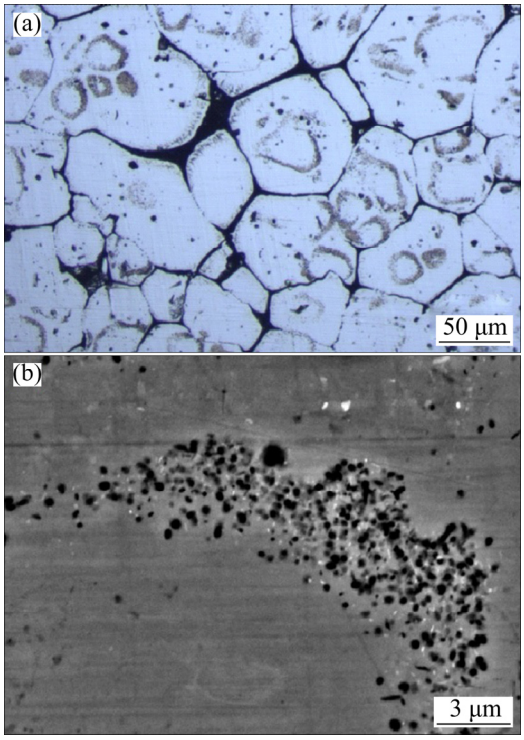


Fig. 8 OM (a) and SEM (b) images of traces (60°, 30 min reheated sample)

In particular, as can be seen from the SEM image, these traces have an ultra-fine mixed particle-like morphology. EDS mapping was applied to a region containing these traces from the same sample and the results obtained are shown in Fig. 9. The results show that the traces do not have a more different composition than the rest of the grain. In this case, it can be said that they do not occur as a result of any segregation.

These traces can only be seen in 30 min of reheating and semi-solid forming conditions and this situation gives an idea about their formation.

A significant deformation may not occur in the solid grains, mostly due to the movement of the liquid phase in semi-solid forming. However, considering that much liquid cannot be formed at the reheating time of 30 min, the deformation also has some effect on the solid grains. With this action, ultra-fine liquid droplets are formed in grains and these droplets appear as traces in the microstructure. The loosening of aluminium grains at high temperature in the reheating may also contribute to the formation of these droplets.

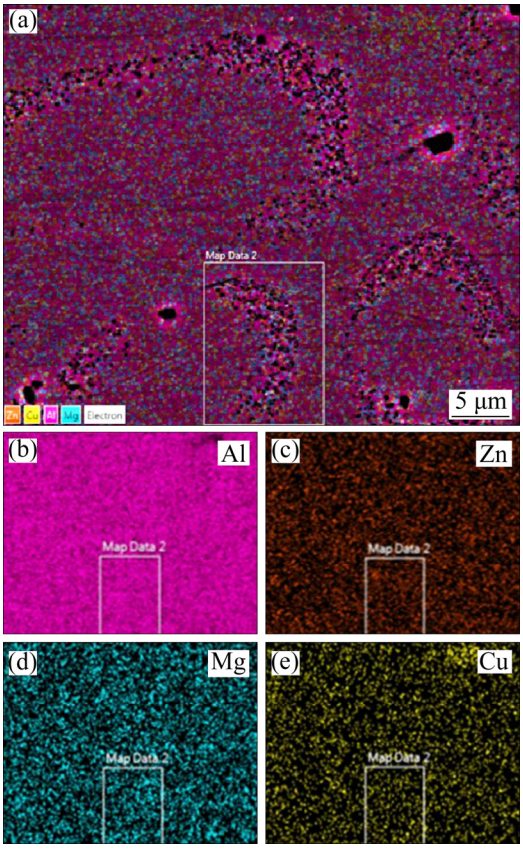


Fig. 9 SEM image (a) and EDS mapping analysis (b−e) of traces seen in Fig. 8(b) (60°, 30 min reheated sample)

4 Conclusions

(1) The cooling slope casting is successful in the production of AA7075 feedstock ingots which have a suitable non-dendritic structure with acceptable grain size for further semi-solid forming processes.

(2) Castings with the slope angle of 60° are superior to 30° castings because they provide both higher casting efficiency and finer grain size.

(3) In the reheating process of the AA7075, grain growth occurs suddenly and very quickly after the formation of the liquid network at the grain boundaries. Therefore, depending on the workpiece size and the heating technique, the time and temperature of the reheating must be determined very carefully.

(4) Although the great effect of reheating on the sphericity is not seen, it can be said that 60° castings are also good in this aspect.

(5) The composition of the liquid phase in the reheating process is different from that of the solid and is rich in copper.

(6) Following the short reheating periods, semi-solid forging causes trace formation in the solid grains.

References

[1] CONG Fu-guan, ZHAO Gang, JIANG Feng, TIAN Ni, LI Rui-feng. Effect of homogenization treatment on microstructure and mechanical properties of DC cast 7X50 aluminum alloy [J]. Transactions of Nonferrous Metals Society of China, 2015, 25: 1027−1034.

[2] ZOU Xiu-liang, YAN Hong, CHEN Xiao-hui. Evolution of second phases and mechanical properties of 7075 Al alloy processed by solution heat treatment [J]. Transactions of Nonferrous Metals Society of China, 2017, 27: 2146−2155.

[3] LIU Tao, HE Chun-nian, LI Gen, MENG Xin, SHI Chun-sheng, ZHAO Nai-qin. Microstructural evolution in Al−Zn−Mg−Cu−Sc−Zr alloys during short-time homogenization [J]. International Journal of Minerals, Metallurgy and Materials, 2015, 22: 516−523.

[4] OZER G, KARAASLAN A. Properties of AA7075 aluminum alloy in aging and retrogression and reaging process [J]. Transactions of Nonferrous Metals Society of China, 2017, 27: 2357−2362.

[5] OZER G, KARAASLAN A. Relationship of RRA heat treatment with exfoliation corrosion, electrical conductivity and microstructure of AA7075 alloy [J]. Materials and Corrosion, 2017, 68: 1260−1267.

[6] SUN Yi-shan, JIANG Fu-lin, ZHANG Hui, SU Jian, YUAN Wu-hua. Residual stress relief in Al−Zn−Mg−Cu alloy by a new multistage interrupted artificial aging treatment [J]. Materials and Design, 2016, 92: 281−287.

[7] BOLOURI A, SHAHMIRI M, CHESHMEH E N H. Microstructural evolution during semisolid state strain induced melt activation process of aluminum 7075 alloy [J]. Transactions of Nonferrous Metals Society of China, 2010, 20: 1663−1671.

[8] BINESH B, AGHAIE-KHAFRI M. Microstructure and texture characterization of 7075 Al alloy during the SIMA process [J]. Materials Characterization, 2015, 106: 390−403.

[9] KUND N K, DUTTA P. Numerical simulation of solidification of liquid aluminum alloy flowing on cooling slope [J]. Transactions of Nonferrous Metals Society of China, 2010, 20: 898−905.

[10] ZHU Wen-zhi, MAO Wei-min, TU Qin. Preparation of semi-solid 7075 aluminum alloy slurry by serpentine pouring channel [J]. Transactions of Nonferrous Metals Society of China, 2014, 24: 954−960.

[11] ATKINSON H, BURKE K, VANEETVELD G. Recrystallisation in the semi-solid state in 7075 aluminium alloy [J]. Materials Science and Engineering A, 2008, 490: 266−276.

[12] ROGAL L, DUTKIEWICZ J M, ATKINSON H, LITYŃSKA-DOBRZYŃSKA L, CZEPPE T, MODIGELL M. Characterization of semi-solid processing of aluminium alloy 7075 with Sc and Zr additions [J]. Materials Science and Engineering A, 2013, 580: 362−373.

[13] CHEN Gang, ZHANG Yu-min, DU Zhi-ming. Mechanical behavior of Al−Zn−Mg−Cu alloy under tension in semi-solid state [J]. Transactions of Nonferrous Metals Society of China, 2016, 26: 643−648.

[14] LI Ming, LI Yuan-dong, BI Guang-li, HUANG Xiao-feng, CHEN Ti-jun, MA Ying. Effects of melt treatment temperature and isothermal holding parameter on water-quenched microstructures of A356 aluminum alloy semisolid slurry [J]. Transactions of Nonferrous Metals Society of China, 2018, 28: 393−403.

[15] HAGA T, SUZUKI S. Casting of aluminum alloy ingots for thixoforming using a cooling slope [J]. Journal of Materials Processing Technology, 2001, 118: 169−172.

[16] HAGA T, KAPRANOS P. Simple rheocasting processes [J]. Journal of Materials Processing Technology, 2002, 130−131: 594−598.

[17] HAGA T, KAPRANOS P. Billetless simple thixoforming process [J]. Journal of Materials Processing Technology, 2002, 130−131: 581−586.

[18] KUMAR D, MANDAL A, CHAKRABORTY M. Cooling slope casting process of semi-solid aluminum alloys: A review [J]. International Journal of Engineering Research and Technology, 2014, 3: 269−283.

[19] JAVDANI A, POUYAFAR V, AMELI A, VOLINSKY A. Blended powder semisolid forming of Al7075/Al_2O_3 composites: Investigation of microstructure and mechanical properties [J]. Materials and Design, 2016, 109: 57−67.

[20] MESHKABADI R, FARAJI G, JAVDANI A, POUYAFAR V. Combined effects of ECAP and subsequent heating parameters on semi-solid microstructure of 7075 aluminum alloy [J]. Transactions of Nonferrous Metals Society of China, 2016, 26: 3091−3101.

[21] FU Jin-long, YANG Dong, WANG Kai-kun. Correlation between the liquid fraction, microstructure and tensile behaviors of 7075 aluminum alloy processed by recrystallization and partial remelting (RAP) [J]. Metals, 2018, 8: 1−15.

[22] CHEN G F, JIANG J F, DU Z M, HAN F, ATKINSON H. Hot tensile behavior of an extruded Al−Zn−Mg−Cu alloy in the solid and in the semi-solid state [J]. Materials and Design, 2014, 54: 1−5.

[23] ROKNI M R, ZAREI-HANZAKI A, ABEDI H R, HAGHDADI N. Microstructure evolution and mechanical properties of backward thixoextruded 7075 aluminum alloy [J]. Materials and Design, 2012, 36: 557−563.

[24] MOHAMMADI H, KETABCHI M, KALAKI A. Microstructure evolution of semi-solid 7075 aluminum alloy during reheating process [J]. Journal of Materials Engineering and Performance, 2011, 20: 1256−1263.

[25] FU Jin-long, JIANG Hong-jun, WANG Kai-kun. Influence of processing parameters on microstructural evolution and tensile properties for 7075 al alloy prepared by an ECAP-based SIMA process [J]. Acta Metallurgica Sinica, 2018, 31: 337−350.

[26] JIANG J F, WANG Y, XIAO G F, NIE X. Comparison of microstructural evolution of 7075 aluminum alloy fabricated by SIMA and RAP [J]. Journal of Materials Processing Technology, 2016, 238: 361−372.

[27] GUNER A T, DISPINAR D, TAN E. Microstructural and mechanical evolution of semisolid 7075 Al alloy produced by SIMA process at various heat treatment parameters [J]. Arabian Journal of Science and Engineering, 2018, 44: 1243−1253.

[28] ATKINSON H, LIU D. Microstructural coarsening of semi-solid aluminium alloys [J]. Materials Science and Engineering A, 2008, 496: 439−446.

[29] CHAYONG S, ATKINSON H, KAPRANOS P. Thixoforming 7075 aluminium alloys [J]. Materials Science and Engineering A, 2005, 390: 3−12.

冷却倾斜板铸造、再加热和触变锻造 AA7075 铝合金

Kerem Altug GULER[1], Alptekin KISASOZ[1], Gokhan OZER[2], Ahmet KARAASLAN[1]

1. Department of Metallurgical and Material Engineering, Yildiz Technical University, TR34210, Istanbul, Turkey;
2. Aluminium Test, Training and Research Center (ALUTEAM), Fatih Sultan Mehmet Vakif University, TR34445, Halic Campus, Istanbul, Turkey

摘　要：冷却倾斜板铸造已成功应用于生产非枝晶组织铝合金的铸造中。为了研究半固态铸造对 AA7075 铝合金显微组织的影响，用冷却倾斜板浇铸法制备具有非枝晶组织的 AA7075 铸锭，并对其进行再加热和触变锻造。对铸件进行金相观察、图像分析、扫描电镜和能谱分析。组织分析结果显示，材料的晶粒尺寸和球形度较好。在再加热过程中，晶粒可能突然变粗。冷却倾斜板铸造采用 30°和 60°倾斜角，采用 60°倾斜角的结果更好。此外，短时再加热和半固态锻造致使固态晶粒中微量元素析出。

关键词：半固态合金；冷却倾斜板铸造；触变锻造；AA7075 合金

(Edited by Wei-ping CHEN)